PAPER • OPEN ACCESS

Wetting behavior of textured silicon surfaces- an experimental study
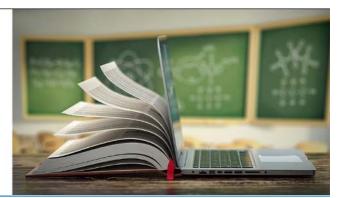
View the article online for updates and enhancements.

Materials Research Express

PAPER

Wetting behavior of textured silicon surfaces- an experimental study

Mohan Kumar K[1,2] and V Velmurugan[2]

1 Dr T. Thimmaiah Institute of Technology, KGF—563120, Karnataka, India
2 Centre for Nanotechnology Research (CNR), VIT- University, Vellore - 632014, Tamil Nadu, India

E-mail: itismohank@gmail.com

Abstract

The behavior of a liquid on a solid surface has shown great interest in a variety of applications related to surfaces and its interfaces. In this paper, the wetting behavior of DI water on micropatterned silicon surfaces fabricated through photolithography and deep reactive ion etching (DRIE) is investigated. Micro pillars of both solid and hollow geometries at a varying pitch and its arrangement in an array has been examined with static contact angle measurement. However, the results concluded that the arrangement of pillars in an array plays an important role as hollow geometries in the case of chain type arrangement provide both hydrophilic and hydrophobic surface properties, while the same hollow geometries in case of zig-zag orientation experiences only hydrophobicity at a varying pitch. Decreased WCA with increased pitch has been observed in the case of a zig-zag arrangement, due to the effect of capillary and gravitation forces. Also the existence of air pockets at sharp corner in the case of hollow square assists in providing maximum contact angle (WCA = 144°) as compared to hollow circle and solid geometries; thus a non-sticky behavior would be possible between the droplet and the patterned surface, due to less adhesion force.

1. Introduction

The advancement in nanotechnology over the last few decades has led to the development of new materials in the field of MEMS / NEMS devices. These devices generally work under extremely light loads and they have a large surface to volume ratio, hence surface properties and surface forces play a vital role in affecting the efficiency and life of the devices. MEMS devices with moving parts such as the microactuators are not yet been commercialized, due to high surface forces associated with friction/stiction and adhesion forces [1].

Wettability commonly referred as an important surface property, is another issue affecting the tribological properties at the micro/nanoscale. The degree to which the solid surface repels a liquid has evoked many industries and academic researches to work in the field of microfluidics, thin-film technology, aerospace components, anti-corrosive, anti-snow sticking and self-cleaning surfaces applications. The wetting of the solid surface by the liquid behavior depends on two main properties of the solid surface under study: the surface energy of the top molecular layer and its surface morphology. Certain studies mention that hydrophobicity can be achieved only by modifying the chemical composition by lowering surface energy [2–10]. However for superhydrophobicity, surface morphology has a significant effect on wettability [11] where the air gets trapped in between the liquid and the rough surface. Thus superhydrophobicity arises from the combination of low surface energy materials and hierarchical or multiscale structure with micro and nano features [12, 13]. Nature has gifted us the combination of these two properties for liquid super repellency in the form of plant Leaves [14] (lotus, Indian canna, knotweed, and taro leaf) and in some insect wings like dragonfly, butterfly, cicada, damselfly, and legs of a water strider.

Two distinct regimes occur when a liquid droplet is placed on micropatterned surfaces. If a droplet penetrates into the gaps of the micropillar termed as wetted regime (static water contact angle WCA < 90°), while if the droplet sits on top of the micropillar supported by entrapped air then it is known as non-wetted regime (WCA > 90°). Wetted regimes usually occurs on hydrophilic surfaces as they possess high surface energy, supporting high friction and adhesion. On the contrary, non-wetted regimes occur on hydrophobic surfaces as they possess low friction and low adhesion because of low surface energy [15].

There is enormous research been conducted by measuring static contact angle on artificial roughened surfaces referred to as micropatterns. 3D negative fingerprint and honeycomb textured surface were fabricated on SU8 coated silicon surface to produce a WCA of 81° and 95° respectively [16], Replicated epoxy micropillars of cylindrical type created by soft lithography provides a CA of 151° [17], SU8 micropillars of square shape were fabricated on silicon by UV lithography achieves a WCA of 131° [18], Micro/nano grooves of varying pitch on silicon wafers by photolithography techniques produces a max contact angle of 48° [15], SU8 microdot patterns were fabricated by polymer jet printing on silicon samples by varying the distance between the dot (pitch) and found that SU8 textured surfaces have shown lower contact angle compared to spin-coated samples (SU8/Si) because of increased exposure of silicon surface [19]. Nanopatterns of PMMA with three different aspect ratios (holding time) were fabricated on silicon surfaces using simple capillary force lithography produced a contact angle of 99° [20]. Silicon micropillars and channels were fabricated using photolithography and deep reactive ion etching (DRIE) Techniques produces a WCA of 59 and 63 respectively [21].

Apart from the geometric parameters being mentioned, there are other factors influencing the wetting behavior, one such is the orientation of the pillars. To the best knowledge of the author, the effect of contact angle on the arrangement of micropillars in an array has not been investigated before; apart from the effect of hollow geometries in comparison with solid geometries. The micropatterns used in the study are an array of circular and square pillars of both solid and hollow cross-section, with uniform height and constant cross-section area, arranged in two different arrangements (chain-type and zig-zag type) at a varying pitch. If the pillars in the adjacent row are opposite to each other then it's termed as chain-type arrangement (figures 2(a)–(d)), and if the pillars are staggered in such a way that every pillar is in the middle of the two pillars of the adjacent rows (figures 2(e), (f)), then the arrangement is said to be zig-zag. But in the zig-zag arrangement, the contact angle measurement depends on the direction of viewing as the patterned surface is no longer Isotropic. This direction dependency called anisotropic wetting behavior can be observed in some natural surfaces like in the case of rice leaves [22], which has the capability to control the water movement in a particular direction [23]. Hence in this paper care was taken to view the static contact angle in the vertical direction (y) and is only been reported (figure 6), as the wetting behavior was slightly different in the horizontal direction (x) [24].

2. Experimental Methodology

2.1. Fabrication of silicon micropatterns
P-type polished silicon of orientation $<100>$, with a thickness of 525μm, was used as a substrate (procured from Prolyx microelectronics pvt ltd—India). Single crystal silicon used traditionally as a structural material is hydrophilic in nature. In this study, micropatterns on a silicon wafer were fabricated using direct-write lithography and deep reactive ion etching (DRIE) technique, as they provide the freedom of shapes with high resolution, smooth surface without any burrs [25].

Figure (1) shows the steps involved in the fabrication process. As an initial step, silicon wafer as received were cleaned sequentially with piranha (H_2SO_4 & H_2O_2 in 3: 1 ratio) solution at 90°C for a duration of 10 min to remove any contamination followed by dipping in dilute hydrofluoric acid (DI water and HF in 50:1) for 30 seconds for native oxide removal, finally the samples were dried with nitrogen gas and the excess moisture on the wafer surface was removed by keeping the wafer on the hot plate at 110°C for 10 min.

The cleaned wafers were then spin-coated with positive photoresist (AZ-4562) and prebaked at 110°C for 75 sec. Micropatterns (array of pillars distributed in a square of 10 × 10mm size on 4 inch silicon wafer) of different geometries by varying the pitch (space between two adjacent pillars) and arrangement (chain and zig-zag) were designed using cleWin software, and the same was developed on the photoresist using a maskless direct write lithography tool (Heidelberg Instrument). DRIE was done as per the Bosch process using two gases (SF_6 and C_4F_8) in a switched/ cyclic process to obtain patterns on the silicon wafer. Finally, the photoresist was removed, and the patterned wafer was sequentially cleaned in acetone, isopropyl alcohol and DI water followed by blowing it with nitrogen gas. The wafer was then diced to 10 × 10mm sample, and each sample has an array of different geometry features fabricated on it for a varied pitch (45, 55, 65 & 75μm).

Table 1 briefs us the details of sample geometries, dimensions and the distance between the consecutive pillars (pitch).

2.2. Surface characterization
Goniometer (Holmarc Opto mechatronics Pvt Ltd) was used to determine the contact angle measurement by gently landing a droplet of de-ionized water (DI) on the test sample from the microsyringe attached to it. Prior to contact angle measurement the samples were immersed in acetone, isopropyl alcohol sequentially and finally washed with DI water and dried by blowing nitrogen gas. A droplet of 5μl volume (diameter of a spherical droplet is around 2.1 mm [26]) was chosen to ensure that the droplet size is comparatively larger than the
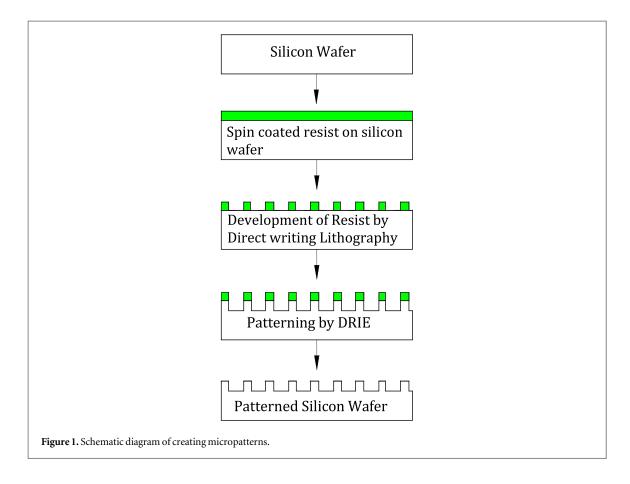
Figure 1. Schematic diagram of creating micropatterns.

Table 1. Dimensions and Geometry of patterns.

Feature	Dimensions of Pillar in μm	Cross-section area of Pillars in μm (A)	Height of Pillar in μm (H)	Pitch in μm (P)
Solid Circle	$D \simeq 31.5$	$\simeq 780$	$14 - 15$	$45, 55, 65 \,\&\, 75$
Hollow Circle	$D_o \simeq 36, D_i \simeq 18$			
Solid Square	$S \simeq 28$			
Hollow Square	$S_o \simeq 32, S_i \simeq 16$			

dimensions of the patterns on the sample. Care was taken to place the droplet on the surface at zero velocity without causing the water droplet to penetrate in between the pillars. The data specified are the average of five readings taken at different locations on the test sample at room temperature, and the standard deviations was calculated and were indicated as error bars.
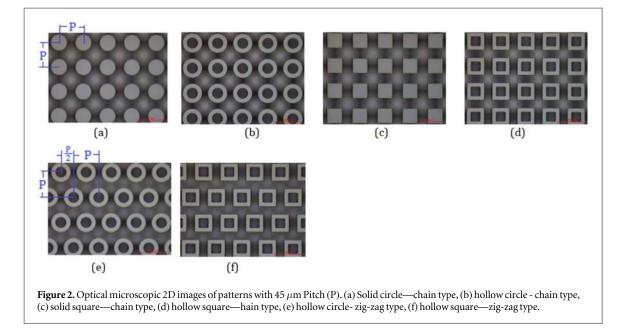
Optical Microscope (Olympus BX61) and Optical Profilometer (Talysurf CCI - Taylor Hobson Precision) was used to examine the exact shape of the micropattern geometry on the fabricated samples. Figure (2) illustrates the 2D optical images and figure (3) shows the surface profile and 3D images of an array of different geometry patterns at 45μm pitch fabricated on the silicon sample.

3. Results and Discussion

Wettability governed by topography has a strong influence on properties of a textured surface, in this study contact angle of the water droplet on the sample is measured to obtain an understanding of the effect of geometry (micropattern) and its arrangement. Hence a comparative study is been made as follows.

3.1. Solid patterns (Chain type) and Hollow patterns (Chain type)
Figure (4) shows the static contact angle as a function of varying pitch for an array of patterns (solid circle, hollow circle, solid square, and hollow square). In this case, both solid and hollow pillars are arranged in a chain type. The graph plotted shows that texturing the silicon surfaces has an effect on the contact angle, as un-textured silicon surfaces have 64° contact angle [27]. Interestingly solid pillars have shown a different plot compared to hollow pillars for both the geometries (circular and square patterns). Hydrophobicity (WCA $>$ 90°) is achieved
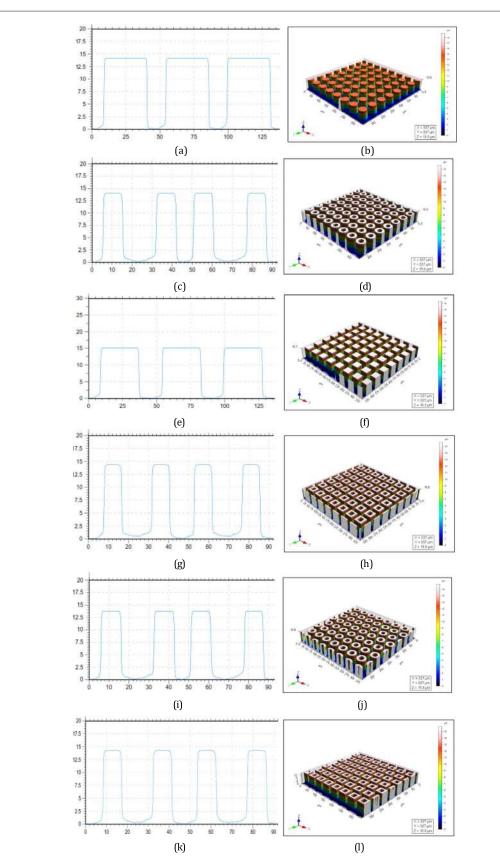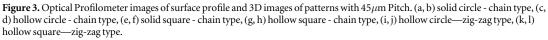
Figure 2. Optical microscopic 2D images of patterns with 45 μm Pitch (P). (a) Solid circle—chain type, (b) hollow circle - chain type, (c) solid square—chain type, (d) hollow square—hain type, (e) hollow circle- zig-zag type, (f) hollow square—zig-zag type.

for all pitches in case of solid pillared patterns, compared to hollow pillared which experiences both hydrophilic (WCA $<$ 90°) and hydrophobic surface properties. There was no superhydrophobicity (WCA $>$ 150°) seen in any of the samples as there was only topography modification without any chemical modification of the surfaces. If a water droplet is landed on the textured samples consisting of pillars arranged in a square grid as in case of chain type, the maximum droop of the droplet occurs in the center of the square formed by four pillars or in between the two pillars which are diagonally across [26] as shown in figure (5a).

In the case of all micropillared surfaces of chain type (solid or hollow) at the lowest and largest pitch, the contact angle is less compared to the intermediate pitch, this is in accordance with [28] that the droplet bounces off on all micropillared surfaces except on the ones fabricated with lowest and highest pitch. This could be due to minimal gap between the pillars in case of lowest pitch (P-45) which is not sufficient for a droplet to bounce [28], as there is minimum/no possibility for air to interfere in between the liquid and solid interface so as to support the liquid droplet. Another reason could be the effect of sharp edges on the pillars at lowest pitch as compared to flat surfaces [26, 29]. Whereas at largest pitch (P-75) there is sufficient space between pillars, such that the liquid droplet penetrates partially/fully between the pillars leaving minimum/no air pockets. In other words the droplet is unable to pull the penetrated liquid and leads to non-bouncing [28]. Also in some cases if the pitch is large, the droplet might not touch the bottom of the cavities, the droplet becomes unstable as it would have entered metastable state resulting in a transition from cassie baxter to wenzel regime [28, 30].

At intermediate pitch (P-55 and P-65) the contact angle is more in all pillared patterns because there is a possibility of air been entrapped in between the liquid and solid surfaces. Also due to sharp corners experienced by solid square-patterned surfaces (SS—CT); for all pitch, the contact angle values are less compared to solid circle patterned surfaces (SC—CT). Therefore for solid circular patterns, the optimum pitch is at P-65, which leads to more contact angle compared to P-55. Also, we can observe from figure (4), that there was a sudden drop in contact angle from P-55 to P-65 in case of solid square patterns, and the droplet which was bouncing (due to more contact angle) lost its stability after few seconds. This is in comparison with square pattern of hollow cross-section at pitch P-65, which has resulted in more contact angle. The inner and outer profile of hollow square have supported the droplet resulting in more contact angle at an optimum pitch P-65, while for solid square at the same pitch the droplet was not supported and instead the droplet becomes unstable.

As described earlier from figure (4), hollow patterned surfaces experience both hydrophilic and hydrophobic characteristics. The hydrophilic state is achieved at the lowest pitch (P-45) as well as at the highest pitch (P-75), whereas at intermediate pitch (P-55 and P-65) the patterned surfaces experience hydrophobic state. Hollow pillars experience a sudden transition from wetting to non-wetting and non-wetting to wetting [28] at the lowest and highest pitch as compared to solid pitch, and the reason would be due to the fixed gap (figure 5(c)), in addition to space (pitch) provided between pillars. The fixed gap and the variable space (pitch) between the pillars assists in both hydrophilic and hydrophobic transitions. The combination of a fixed gap and lowest pitch, fixed gap and largest pitch between pillars have led to the lowest contact angle (hydrophilicity), whereas intermediate pitch in combination with fixed gap leads to hydrophobicity. The values of contact angle at the intermediate pitch for hollow patterned surfaces are more compared to solid pillars, this is due to the addition of a fixed gap making the water droplet to bounce on the pillars. Therefore hollow pillars at varied pitch enhance

Figure 3. Optical Profilometer images of surface profile and 3D images of patterns with 45 μm Pitch. (a, b) solid circle - chain type, (c, d) hollow circle - chain type, (e, f) solid square - chain type, (g, h) hollow square - chain type, (i, j) hollow circle—zig-zag type, (k, l) hollow square—zig-zag type.

both hydrophilic and hydrophobic characteristics compared to solid pillars. As described the sharp corners in the solid square have reduced the values of contact angle in comparison with solid circular patterned surfaces, whereas the same sharp corners that occur at both inner and outer surfaces/ profiles of the hollow square
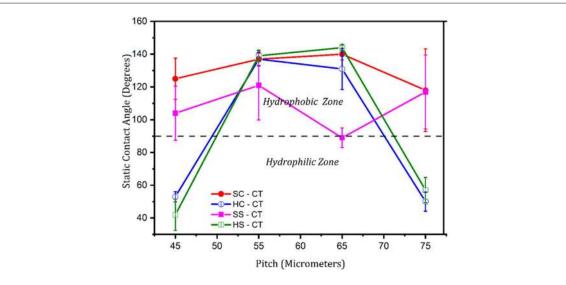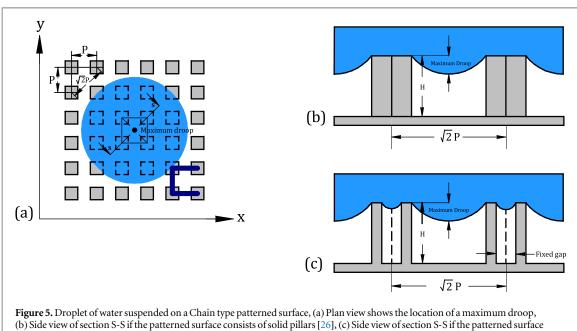
Figure 4. Static contact angle of Solid (chain type) and Hollow (chain type) patterns as a function of varied pitch.

Figure 5. Droplet of water suspended on a Chain type patterned surface, (a) Plan view shows the location of a maximum droop, (b) Side view of section S-S if the patterned surface consists of solid pillars [26], (c) Side view of section S-S if the patterned surface consists of hollow pillars (chain type).
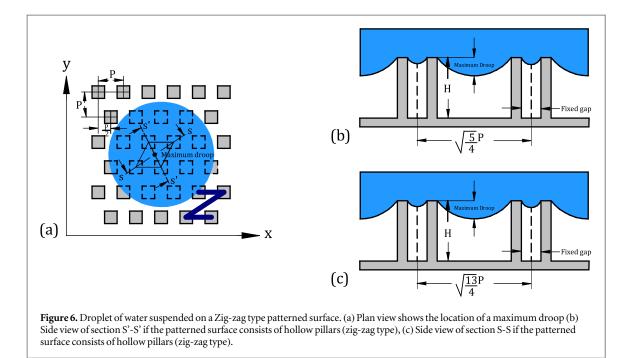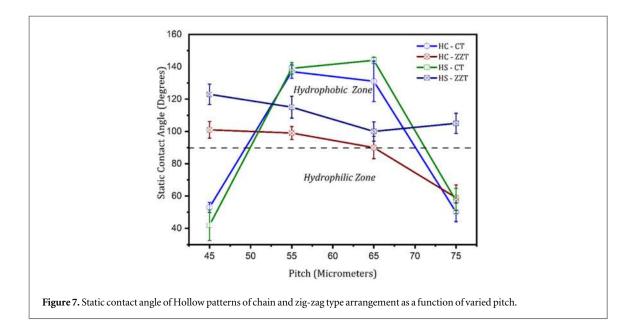
(HS—CT) have increased the contact angle in comparison with hollow circular patterns (HC—CT). Therefore hollow square-patterned surfaces at P-65 have produced more contact angle (WCA = 144) compared to all other patterned surfaces having the same area of cross-section.

3.2. Hollow patterns (Chain type) and Hollow patterns (Zig-zag type)

Figure (7) presents the static contact angle values at a varying pitch for hollow patterns of chain type (CT) and zig-zag type (ZZT) arrangement. In chain type arrangement both hydrophobic and hydrophilicity can be noticed for both the geometries, whereas in zig-zag arrangement except for hollow circle at highest pitch, all the values obtained are in the hydrophobic zone. In case of chain type arrangement, the adjacent row of pillars are opposite to each other as shown in figure (5(a)), hence the maximum droop is at the intersection of the diagonals formed by four pillars in a square grid (distance between the diagonals is $\sqrt{2}P$, where P is pitch between the adjacent pillars); whereas in zig-zag arrangement the adjacent row of pillars is shifted by half the pitch, hence the maximum droop occurs at the intersection of diagonals formed by four pillars placed in a parallelogram. There are two diagonals, minimum and the maximum as shown in figure 6(b), (c)) for section S-S and S'-S' from the figure (6(a)). As mentioned earlier, WCA for a zig-zag arrangement is viewed in the vertical direction (y), and hence from the plot, we can observe that the WCA values are decreased as the pitch increases; this is because of

Figure 6. Droplet of water suspended on a Zig-zag type patterned surface. (a) Plan view shows the location of a maximum droop (b) Side view of section S'-S' if the patterned surface consists of hollow pillars (zig-zag type), (c) Side view of section S-S if the patterned surface consists of hollow pillars (zig-zag type).

Figure 7. Static contact angle of Hollow patterns of chain and zig-zag type arrangement as a function of varied pitch.

the large distance between the pillars diagonally $= \sqrt{\left(\left(\frac{13}{4}\right)\right)}P$, where the liquid-air interface is destabilized leading to the formation of the solid-liquid interface due to capillary and gravitational forces [26]. From this, we can observe that the arrangement of pillars/patterns in an array plays a predominant role in the measurement of the water contact angle. Also, the highest contact angles can be achieved by hollow square as compared to the hollow circle in both the arrangement, as the air pockets exists in the sharp corners in case of hollow squares at both inner and outer surface and this could be the valid reason for a water droplet to bounce on the pillars [31].

From the above study been observed, when a water droplet falls on a roughened/micropatterned surfaces, the wetting behavior of a liquid can be explained either by the Wenzel model or by Cassie Baxter model.

According to Wenzel model, when a water droplet completely wets the textured surfaces; the contact angle is given as

$$\cos \theta_w = r \cos \theta \tag{1}$$

where θ_w is the WCA on the micro-patterned surface in Wenzel state, r is the surface roughness factor which is defined as the ratio of the actual area of a rough surface to the projected area., and θ is WCA on a flat surface of the same material (Young's contact angle).

In contrast, the patterned surfaces (except hollow geometries at lowest and highest pitch in case of chain-type arrangement) have a larger contact angle compared to bare silicon which experiences hydrophilicity (WCA < 90°). This indicates that the WCA on micropatterned surfaces is characterized by the Cassie-Baxter model rather than the Wenzel model [32].

Therefore according to Cassie-Baxter model, for a liquid droplet that sits on top of the micropillar supported by entrapped air have low adhesive force, and the contact angle is given as

$$\cos \theta_c = f_s(1 + \cos \theta) - 1 \tag{2}$$

where θ_c is the WCA on the micro-patterned surface in cassie baxter state, f_s is the fraction of the solid in contact with the liquid droplet, hence the equation shows that the contact angle increases as the solid fraction decreases in Cassie state. However in few studies, the liquid droplet partially enters the patterned surface leading to an intermediate wetting model [31, 33] and this could be evaluated by measuring the sliding angle [32]. Thus texturing is an effective way to improve the wetting behavior by reducing the surface real area of contact, and further can be enhanced by combining with chemical modification [15, 18, 34].

4. Conclusion

An investigation on the effect of texture geometry and its arrangement in an array was carried out using a droplet of DI water under static conditions. Circular and square were the geometries selected for fabricating patterns with both hollow and circular cross-sections. The patterns were arrangement in both chain type and zig-zag type. The results concluded that texturing has an effect on contact angle measurement. At the varying pitch in the chain-type arrangement, solid patterns have resulted in hydrophobicity, whereas hollow patterns experience both hydrophilic and hydrophobicity; the addition of a fixed gap could be a valid reason. Hollow square in the chain-type arrangement has a large contact angle (WCA = 144°) at pitch 65 μm compared to other geometries and cross-section, this may be due to existence of air pockets at the sharp corners that occur at both inner and outer surfaces, which makes the water droplet to bounce on the pillars leading to less adhesive force. Pattern arrangement plays a crucial role, zig-zag arrangement has WCA less than the chain type arrangement for hollow patterns, this is because of forces influenced by gravitation and capillary at large diagonal distance between the pillars leading to the homogeneous solid-liquid interface.

ORCID iDs

Mohan Kumar K ● https://orcid.org/0000-0001-5165-0423
V Velmurugan ● https://orcid.org/0000-0001-7893-4514

References

[1] Kumar K M, Shanmuganathan P V and Sethuramiah A 2018 Tribology of silicon surfaces: a review *Materials Today: Proceedings* **5** 24809–19

[2] Nishino T, Meguro M, Nakamae K, Matsushita M and Ueda Y 1999 The lowest surface free energy based on— CF3 alignment *Langmuir* **15** 4321–3

[3] Cha K H and Kim D E 2001 Investigation of the tribological behavior of octadecyl trichlorosilane deposited on silicon *Wear* **251** 1169–76

[4] Satyanarayana N, Sinha S K and Ong B H 2006 Tribology of a novel UHMWPE/PFPE dual-film coated onto Si surface *Sens. Actuators, A* **128** 98–108

[5] Ma J Q, Pang C J, Mo Y F and Bai M W 2007 Preparation and tribological properties of multiply-alkylated cyclopentane (MAC)– octadecyl trichlorosilane (OTS) double-layer film on silicon *Wear* **263** 1000–7

[6] Minn M and Sinha S K 2008 DLC and UHMWPE as hard/soft composite film on Si for improved tribological performance *Surf. Coat. Technol.* **202** 3698–708

[7] Saravanan P, Satyanarayana N and Sinha S K 2013 Self-lubricating SU-8 nanocomposites for microelectromechanical systems applications *Tribol. Lett.* **49** 169–78

[8] Panjwani B, Satyanarayana N and Sinha S K 2011 Tribological characterization of a biocompatible thin film of UHMWPE on Ti6Al4V and the effects of PFPE as a top lubricating layer *J. Mech. Behav. Biomed. Mater.* **4** 953–60

[9] Minn M, Soetanto Y S and Sinha S K 2011 Tribological properties of ultra-thin functionalized polyethylene film chemisorbed on Si with an intermediate benzophenone layer *Tribol. Lett.* **41** 217–26

[10] Chen H, Zhang X, Zhang P and Zhang Z 2012 Facile approach in fabricating superhydrophobic SiO2/polymer nanocomposite coating *Appl. Surf. Sci.* **261** 628–32

[11] Ogihara H, Xie J and Saji T 2013 Factors determining wettability of superhydrophobic paper prepared by spraying nanoparticle suspensions *Colloids Surf., A* **434** 35–41

[12] Verho T, Korhonen J T, Sainiemi L, Jokinen V, Bower C, Franze K and Ras R H 2012 Reversible switching between superhydrophobic states on a hierarchically structured surface *Proc. of the National Academy of Sciences* 109, 10210–3

[13] Papadopoulos P, Mammen L, Deng X, Vollmer D and Butt H J 2013 How superhydrophobicity breaks down *Proc. of the National Academy of Sciences* 110, 3254–8

[14] Guo Z and Liu W 2007 Biomimic from the superhydrophobic plant leaves in nature: Binary structure and unitary structure *Plant Science* **172** 1103–12

[15] Wang Y, Wang L, Xue Q, Yuan N and Ding J 2010 A facile method to improve tribological properties of silicon surface by combining nanogrooves patterning and thin-film lubrication *Colloids Surf., A* **372** 139–45

[16] Myint S M, Minn M, Yaping R, Satyanarayana N, Sinha S K and Bhatia C S 2013 Friction and wear durability studies on the 3D negative fingerprint and honeycomb textured SU-8 surfaces *Tribol. Int.* **60** 187–97

[17] Ebert D and Bhushan B 2012 Durable Lotus-effect surfaces with hierarchical structure using micro-and nanosized hydrophobic silica particles *J. Colloid Interface Sci.* **368** 584–91

[18] Milionis A, Bayer I S, Fragouli D, Brandi F and Athanassiou A 2013 Combination of lithography and coating methods for surface wetting control In Updates in Advanced Lithography. IntechOpen

[19] Tay N B, Minn M and Sinha S K 2011 Polymer jet printing of SU-8 micro-dot patterns on Si surface: optimization of tribological properties *Tribol. Lett.* **42** 215

[20] Yoon E S, Singh R A, Kong H, Kim B, Kim D H, Jeong H E and Suh K Y 2006 Tribological properties of bio-mimetic nano-patterned polymeric surfaces on silicon wafer *Tribol. Lett.* **21** 31–7

[21] Singh R A, Pham D C, Kim J, Yang S and Yoon E S 2009 Bio-inspired dual surface modification to improve tribological properties at small-scale *Appl. Surf. Sci.* **255** 4821–8

[22] Feng L, Li S, Li Y, Li H, Zhang L, Zhai J and Zhu D 2002 Super-hydrophobic surfaces: from natural to artificial *Adv. Mater.* **14** 1857–60

[23] Wu D, Wang J N, Wu S Z, Chen Q D, Zhao S, Zhang H and Jiang L 2011 Three-level biomimetic rice-leaf surfaces with controllable anisotropic sliding *Adv. Funct. Mater.* **21** 2927–32

[24] Cassie A B D and Baxter S 1944 Wettability of porous surfaces *Trans. Faraday Soc.* **40** 546–51

[25] Wang X and Kato K 2003 Improving the anti-seizure ability of SiC seal in water with RIE texturing *Tribol. Lett.* **14** 275–80

[26] Bhushan B and Jung Y C 2008 Wetting, adhesion and friction of superhydrophobic and hydrophilic leaves and fabricated micro/nanopatterned surfaces *J. Phys. Condens. Matter* **20** 225010

[27] Kashaninejad N, Chan W K and Nguyen N T 2012 Eccentricity effect of micropatterned surface on contact angle *Langmuir* **28** 4793–9

[28] Patil N D, Bhardwaj R and Sharma A 2016 Droplet impact dynamics on micropillared hydrophobic surfaces *Exp. Therm Fluid Sci.* **74** 195–206

[29] Nosonovsky M and Bhushan B 2005 Roughness optimization for biomimetic superhydrophobic surfaces *Microsyst. Technol.* **11** 535–49

[30] Bhushan B, Jung Y C and Nosonovsky M 2010 Lotus effect: surfaces with roughness-induced superhydrophobicity, self-cleaning, and low adhesion *Springer Handbook of Nanotechnology* (Berlin, Heidelberg: Springer) pp 1437–524

[31] Luo C, Xiang M and Heng X 2012 A stable intermediate wetting state after a water drop contacts the bottom of a microchannel or is placed on a single corner *Langmuir* **28** 9554–61

[32] Bae K J, Yao W, He Y and Cho Y R 2017 Wetting behavior of liquids on micro-patterned polymer surfaces fabricated by thermal imprinting *Korean Journal of Metals and Materials* **55** 624–31

[33] Li Z, Wang J, Zhang Y, Wang J, Jiang L and Song Y 2010 Closed-air induced composite wetting on hydrophilic ordered nanoporous anodic alumina *Appl. Phys. Lett.* **97** 233107

[34] Zhao W, Pu J, Yu Q, Zeng Z, Wu X and Xue Q 2013 A novel strategy to enhance micro/nano-tribological properties of DLC film by combining micro-pattern and thin ionic liquids film *Colloids Surf., A* **428** 70–8